nature geoscience

ARTICLES

PUBLISHED ONLINE: 19 JUNE 2017 | DOI: 10.1038/NGEO2974

Abrupt North Atlantic circulation changes in response to gradual CO_2 forcing in a glacial climate state

Xu Zhang[1,2*], Gregor Knorr[1,3], Gerrit Lohmann[1,4] and Stephen Barker[3]

Glacial climate is marked by abrupt, millennial-scale climate changes known as Dansgaard–Oeschger cycles. The most pronounced stadial coolings, Heinrich events, are associated with massive iceberg discharges to the North Atlantic. These events have been linked to variations in the strength of the Atlantic meridional overturning circulation. However, the factors that lead to abrupt transitions between strong and weak circulation regimes remain unclear. Here we show that, in a fully coupled atmosphere–ocean model, gradual changes in atmospheric CO_2 concentrations can trigger abrupt climate changes, associated with a regime of bi-stability of the Atlantic meridional overturning circulation under intermediate glacial conditions. We find that changes in atmospheric CO_2 concentrations alter the transport of atmospheric moisture across Central America, which modulates the freshwater budget of the North Atlantic and hence deep-water formation. In our simulations, a change in atmospheric CO_2 levels of about 15 ppmv—comparable to variations during Dansgaard–Oeschger cycles containing Heinrich events—is sufficient to cause transitions between a weak stadial and a strong interstadial circulation mode. Because changes in the Atlantic meridional overturning circulation are thought to alter atmospheric CO_2 levels, we infer that atmospheric CO_2 levels may serve as a negative feedback to transitions between strong and weak circulation modes.

Abrupt climate changes associated with Dansgaard–Oeschger (DO) events as recorded in Greenland ice cores are characterized by rapid warming from stadial to interstadial conditions. This is followed by a phase of gradual cooling before an abrupt return to cold stadial conditions[1,2]. A common explanation for these transitions involves changes in the Atlantic meridional overturning circulation (AMOC)[3], perhaps controlled by freshwater perturbation (for example, refs 4,5) and/or Northern Hemisphere ice sheet changes (for example, refs 6–8). To reproduce the abrupt transitions into and out of cold conditions across the North Atlantic (that is, AMOC weak or 'off' mode[3]), a common trigger mechanism is related to the timing of North Atlantic freshwater perturbations[9,10] that is mainly motivated by unequivocal ice-rafting events during Heinrich Stadials (HS)[11]. However, recent studies suggest that the Heinrich ice-surging events are in fact triggered by sea subsurface warming associated with an AMOC slow-down[12,13]. Furthermore, the duration of ice-rafting events does not systematically coincide with the beginning and end of the pronounced cold conditions during Heinrich Stadials[14,15]. This evidence thus challenges the current understanding of glacial AMOC stability[5,8], suggesting the existence of additional control factors that should be invoked to explain abrupt millennial-scale variability in climate records. In contrast to the north, the rapid climate transitions are characterized by interhemispheric anti-phased variability, with more gradual changes in southern high latitudes[16] due to the thermal bipolar seesaw effect[17]. This Antarctic-style climate variability[16], represents a pervasive signal on a global scale and shares a close correspondence with changes in atmospheric CO_2 (refs 18,19). In addition, numerous palaeoclimate records clearly show that DO activity is most pronounced when both global ice volume and atmospheric CO_2 levels are intermediate between glacial and interglacial extremes[1,2,6,20,21]. Taken together, this evidence has led to suggestions that gradual changes in background climate, associated with variations in atmospheric CO_2, have the potential to explain the occurrence of abrupt climate shifts during ice ages[18,19,22,23].

Gradual CO_2 changes as a forcing factor

With aid of the comprehensive coupled climate model COSMOS[8,9] we explore the governing mechanism of AMOC stability associated with atmospheric CO_2 changes. Two experiments were conducted with gradual changes in atmospheric CO_2 under intermediate (CO2_Hys) and maximum (LGM_0.15_CO2) ice volumes (Supplementary Table 1). In experiment CO2_Hys, atmospheric CO_2 concentration was linearly changed between 185 and 239 ppm at a rate of 0.02 ppm yr^{-1} to mimic millennial-scale CO_2 variations during glacials[24]. This forcing is sufficiently weak such as to simulate a quasi-equilibrium response of the climate system to changing CO_2. The prescribed (intermediate) ice volume is equivalent to a sea level of ~42 m below present-day conditions[8] (Supplementary Table 1), equivalent to an early stage of the last glacial cycle[25]. Other boundary conditions were kept constant at Last Glacial Maximum (LGM) conditions[9] (Methods).

In experiment LGM_0.15_CO2, an equilibrated weak AMOC mode forced by persistent freshwater flux (0.15 Sv, Sv = 10^6 m^3 s^{-1}) under LGM conditions[9] (Supplementary Table 1) serves as the initial state (Supplementary Fig. 1). The freshwater perturbation can be considered to represent North Atlantic (NA) meltwater input associated with the surface mass balance of the surrounding ice sheets and/or freshwater injection associated with ice-surging events during Heinrich Stadials. The atmospheric CO_2 concentration varies

[1]Alfred Wegener Institute Helmholtz Centre for Polar and Marine Research, Bussestrasse 24, D-27570, Germany. [2]Laboratory for Marine Geology, Qingdao National Laboratory for Marine Science and Technology, Qingdao 266061, China. [3]School of Earth and Ocean Sciences, Cardiff University, Cardiff CF10 3AT, UK. [4]MARUM-Center for Marine Environmental Sciences, University Bremen, Leobener Strasse D-28359, Germany.
*e-mail: xu.zhang@awi.de

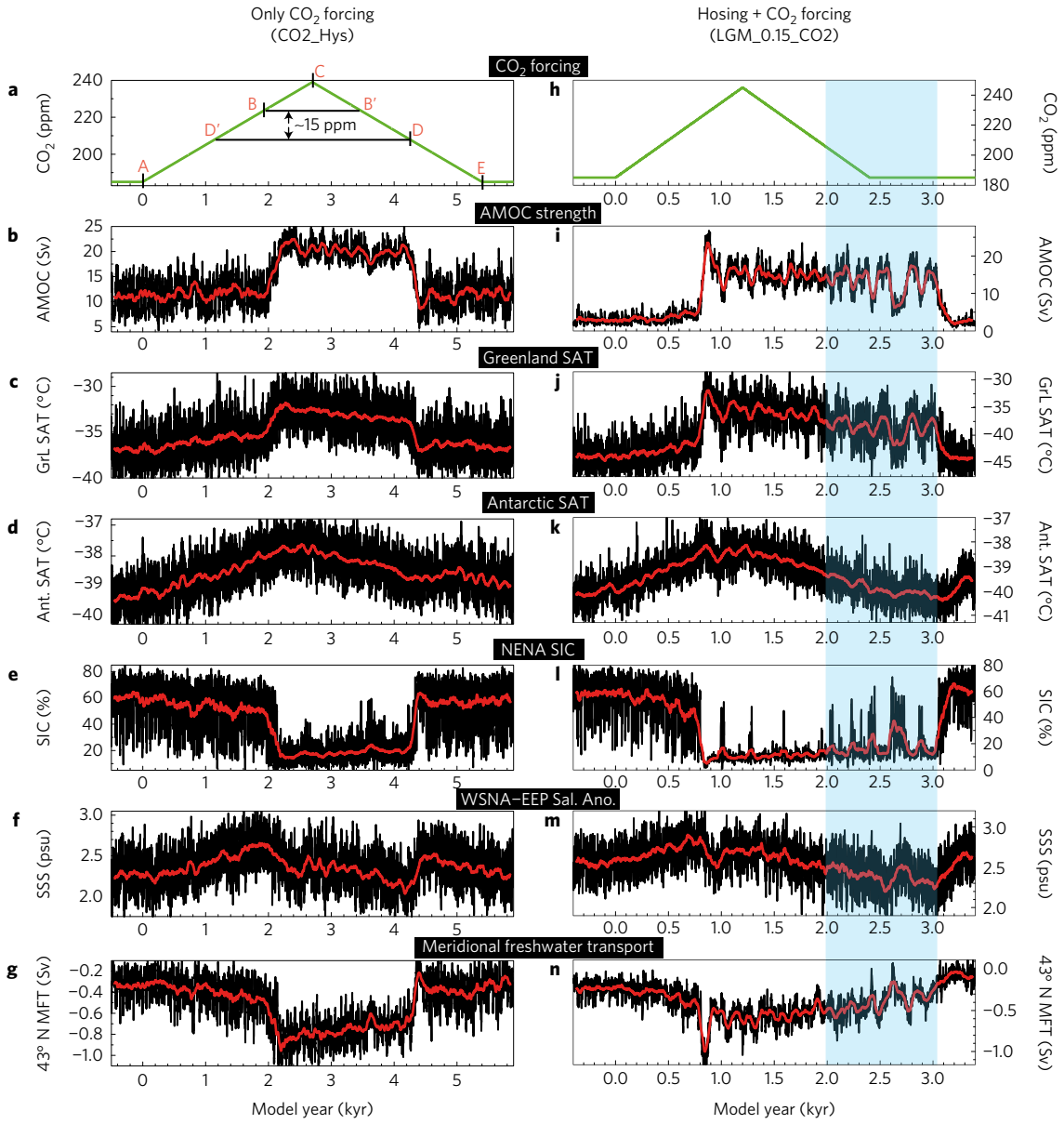

Figure 1 | Transient simulations of the experiment CO2_Hys (left) and LGM_0.15_CO2 (right). a,**h**, CO_2 forcing (ppm). **b**,**i**, AMOC index (Sv). **c**,**j**, Greenland SAT (°C). **d**,**k**, Antarctic (70°–80° S zonal mean) SAT index (°C). **e**,**l**, NENA SIC index (%). **f**,**m**, Sea surface salinity (SSS) anomaly (psu) between the WSNA and EEP. **g**,**n**, AMOC-associated MFT[31] (Sv) across 43° N in the North Atlantic. Thin black lines represent the original modelled outputs, and thick red lines in **b**–**g** and **i**–**n** are the 100-year and 60-year running means, respectively. Negative model years indicate the control simulations.

gradually between 185 ppm and 245 ppm at a rate of 0.05 ppm yr^{-1}, representative of the observed rate of CO_2 changes during the last deglaciation[26]. This set-up provides a surrogate for Heinrich stadial–interstadial transitions during glacial periods (especially during the last deglaciation) to test the robustness of the simulated changes in experiment CO2_Hys. As shown later, in both experiments the AMOC shares similar characteristics in response to the CO_2 changes (Fig. 1).

AMOC response to gradual CO_2 changes

The simulated glacial ocean circulation (prior to transient forcing) is characterized by a weak AMOC mode with cold stadial conditions in the north (Fig. 1a–c). In response to a linear increase in CO_2 concentration, surface air temperature (SAT) over the northern high latitudes experiences abrupt warming, along with a rapid AMOC reorganization from a weak stadial to a strong interstadial mode (interval A–B in Fig. 1a, and Supplementary Fig. 2a). The opposite occurs in the scenario with decreasing atmospheric CO_2 (interval C–D in Fig. 1a, and Supplementary Fig. 2a). The simulated magnitude of abrupt Greenland warming/cooling is much smaller than the observed, probably due to the underestimated sea-ice retreat in the Nordic Seas[27] in the strong AMOC mode of experiment CO2_Hys (Supplementary Fig. 3). Nevertheless, changes in sea surface temperature in the North Atlantic are well captured between the two contrasting climate states (Supplementary Figs 4 and 5). In contrast to the abrupt climate shifts in the north, the simulated Antarctic and global SATs vary more gradually, in line with the CO_2 forcing (Fig. 1a–d and Supplementary Fig. 2a,g). This gradual signature is also reflected in the SAT trend of the northern high latitudes prior to the abrupt transitions (that is, the period A–B and C–D in Fig. 1a and Supplementary Fig. 2a). The AMOC itself does not show this gradual trend, and instead maintains a relatively constant strength before experiencing an abrupt shift (Fig. 1a–c). In addition, it is worth noting that changes in CO_2

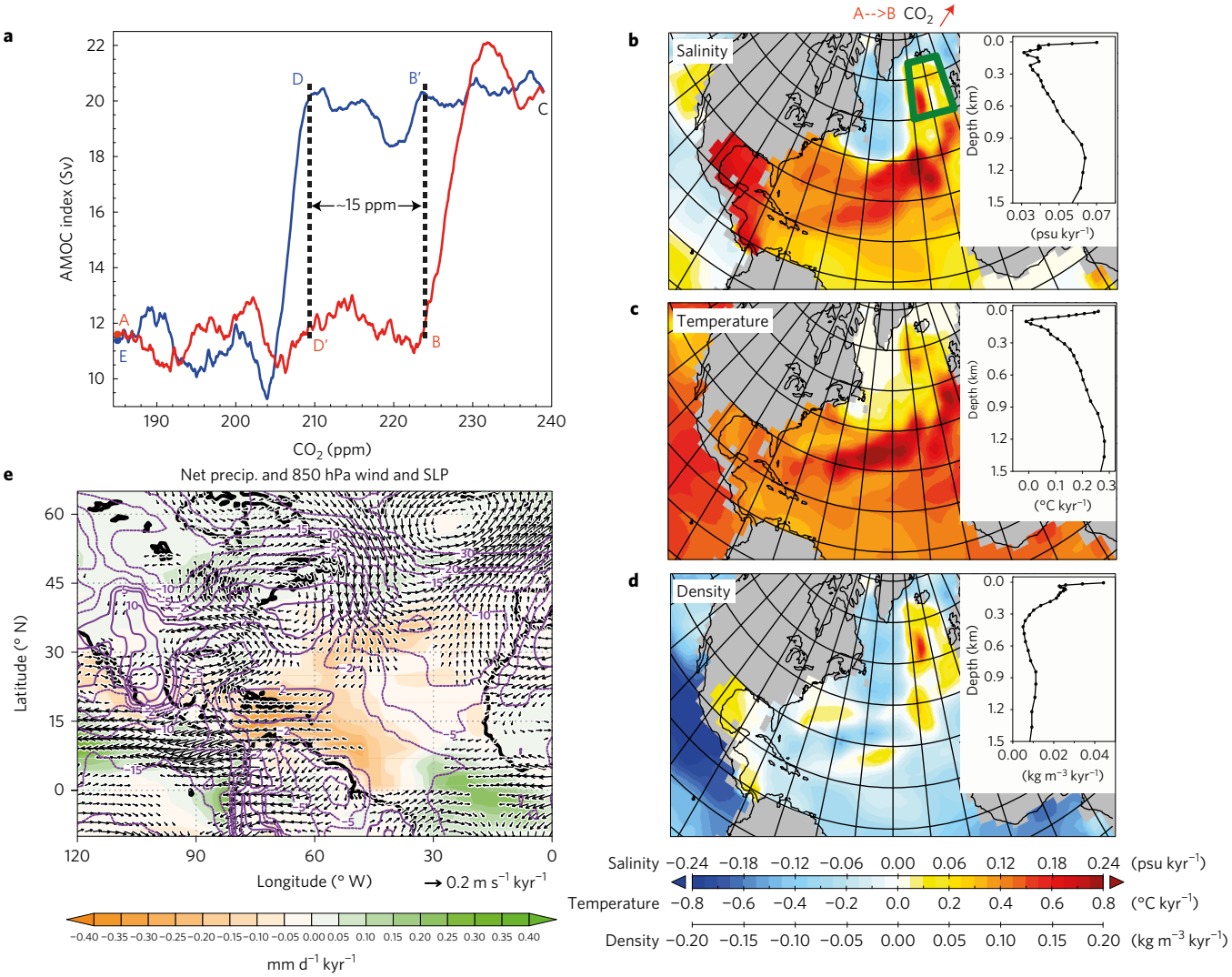

Figure 2 | AMOC hysteresis and trend analysis in the increasing CO_2 scenario of the experiment CO2_Hys. a, AMOC hysteresis associated with CO_2 changes. Time points defined in Fig. 1a are shown by letters, within which point A and E are indicated by red and blue circles, respectively. **b**–**e**, Trend in the CO_2 increasing scenario (interval A–B in **a**). **b**–**d**, Sea surface salinity (psu kyr^{-1}) (**b**), temperature (°C kyr^{-1}) (**c**) and density (kg m^{-3} kyr^{-1}) (**d**), with their vertical profiles over the NENA (as shown by green rectangle in **b**) plotted as insets in the upper-right corner. **e**, Net precipitation (mm d^{-1} kyr^{-1}, shaded), 850 hPa wind (m s^{-1} kyr^{-1}, vector) and sea-level pressure trend (Pa kyr^{-1}, contour).

concentration (~15 ppm) that account for the coexistence of two distinct glacial ocean states (Fig. 2a) are of comparable magnitude as real millennial-scale CO_2 variations recorded during glacial cycles[20,24] (Fig. 1a,b). Overall, the simulated changes (Fig. 1a–e and Supplementary Figs 2–5) share many characteristics with empirical evidence of millennial-scale Heinrich–DO variability[16,20,24,28,29].

We now focus on the first 2000 model years of experiment CO2_Hys while AMOC is in its weak mode to illustrate the underlying dynamics of the abrupt AMOC amplification at the end of interval A–B in Fig. 1a. It is known that the sinking branch of the AMOC closely relates to the vertical stratification (that is, vertical density gradient) that is mainly controlled by ocean temperature and salinity in the main convection sites of the North Atlantic. At the sea surface, the background warming (~0.25 °C kyr^{-1}), which is linked to the CO_2 increase, decreases the surface water density in the northeastern North Atlantic (NENA, the main convection sites, 50°–65° N, 10°–30° W). This strengthens the vertical stratification and thermally stabilizes the weak mode of AMOC (Fig. 2c). Nevertheless, the thermal impact on surface density is overcome by a synchronous haline effect (that is, the surface water salinity increase at a rate of ~0.07 psu kyr^{-1}, see below). This offsets the warming effect and causes a net increase in the surface water density at a rate of ~0.04 kg m^{-3} kyr^{-1} (Fig. 2b,d). This relationship is also detected at the subsurface in the NENA, leading to water density increase at a slower rate (that is, ~0.01 kg m^{-3} kyr^{-1}) than the surface density increase (Fig. 2b,d). This vertical contrast in rates of water density change highlights the importance of a top-down de-stratification via surface salinization, eventually leading to an abrupt AMOC recovery.

Of particular importance to explain the surface salinity increase in the NENA are changes in meridional freshwater transport (MFT) in the North Atlantic[30]. We find that an increase in the northward salinity transport (negative MFT in Fig. 1g) dominates over local surface freshening (~0.0011 Sv kyr^{-1}) associated with increased net precipitation in the NENA (Fig. 2e). Along with the CO_2 increase, the MFT during the weak AMOC phase gradually decreases by ~0.2 Sv across the boundary between the subtropical and subpolar gyre in the North Atlantic (~43° N) prior to the rapid AMOC recovery (Fig. 1g). Since the strength of the AMOC during this interval is relatively stable (Fig. 1b), the weakened MFT can be mainly attributed to an increase in the subtropical sea surface salinity in the North Atlantic (see below). This causes a saltier

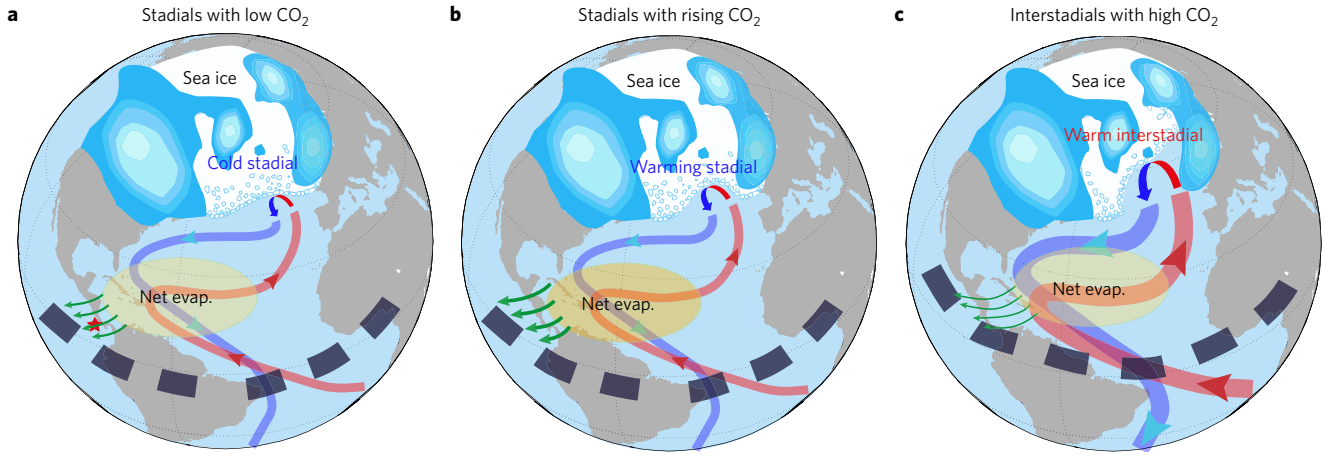

Figure 3 | Summary cartoon of the proposed mechanism in this study. a, Stadial conditions with a relatively low atmospheric CO_2 level. **b**, Stadial conditions with rising CO_2. **c**, Interstadial conditions with a high CO_2 level. Location of the palaeosalinity record[38] is highlighted by the red star in **a**. Dark dashed lines represent the ITCZ. Interoceanic moisture transport is represented by green arrows, of which the thickness schematically indicates the strength of moisture transport. Red and blue belts/arrows indicate the upper northward and deeper southward AMOC branch, respectively. The brown shading represents the net evaporation region over the western subtropical North Atlantic.

northward AMOC branch that feeds into the NENA via the North Atlantic subtropical gyre. Changes in the freshwater import across the southern boundary of the Atlantic catchment area at ~29° S (refs 31,32) and the equatorial Atlantic Ocean are determined to be of minor importance (Supplementary Fig. 2j,k).

A key mechanism responsible for changes in the subtropical sea surface salinity is the zonal atmospheric moisture transport across Central America. Previous data and model studies suggest that a southward shift of the intertropical convergence zone (ITCZ) is responsible for the salinity increase in the western subtropical North Atlantic (WSNA, 60°–90° W, 10°–30° N) during cold stadial periods[28,30,33–35]. This is presumed to be a precondition for North Atlantic Deep Water (NADW) formation to abruptly return to warm interstadial conditions with a strong AMOC mode[28,34]. In our model, the southward-displaced ITCZ (Supplementary Fig. 4b) and salinity increase in the WSNA (Supplementary Fig. 5a) are well captured in the simulated strong-to-weak AMOC transition. However, the salinity increase stops after the transition is complete (Supplementary Fig. 6). As a consequence, the stationary salinity anomaly is not sufficient to enable an abrupt resumption of the AMOC (Fig. 3a), as shown in simulations LIS_0.2 and LGM_0.15 (Supplementary Fig. 1 and Supplementary Table 1) that are, respectively, equivalent to experiments CO2_Hys and LGM_0.15_CO2, but without CO_2 changes.

However, once a CO_2 increase is additionally imposed to the cold stadial conditions (for example, interval A–B in CO2_Hys), trade winds over the Central America are further enhanced by the strengthened sea-level pressure gradient between the eastern equatorial Pacific (EEP, 90°–120° W, 5°–15° N) and the WSNA (Figs 2e and 3b). This is a consequence of the associated El Niño-like warming pattern in the Pacific and Atlantic with a relatively stronger warming in the EEP than the WSNA (Supplementary Fig. 7). These warming characteristics are consistent with sea surface temperature responses in global warming scenarios as simulated in climate projections using CMIP5 models[36]. In addition to increased evaporation over the WSNA due to the Clausius–Clapeyron relation, the enhanced trade winds boost the atmospheric moisture transport, reducing (increasing) surface water salinity in the EEP (WSNA) (Fig. 1f and Supplementary Fig. 2h,i).

To further test this, we analyse the observed CO_2-$Salinity_{EEP}$ relationship during Heinrich Stadial intervals that are accompanied with CO_2 increases in the past 90 thousand years[20,37,38] (Supplementary Figs 8 and 9). As shown in Supplementary Fig. 10, rising CO_2 did appear to coincide with declining salinity in the EEP[38] (Supplementary Fig. 9). These findings thus suggest that changes in the atmospheric moisture transport across Central America, driven by a gradual CO_2 increase, can stimulate an AMOC recovery from cold Heinrich Stadial conditions by increasing salinity in the subtropical North Atlantic (Fig. 3b,c). This also reconciles previous controversies regarding the roles played by the southward-shifted ITCZ during cold Heinrich stadials on the subsequent abrupt transitions to warm interstadials[28,34,38].

In addition to the haline impact, decline in sea-ice concentration (SIC) in the North Atlantic, as a positive feedback to AMOC recovery[8], helps to reinforce abrupt AMOC changes. In CO2_Hys the reduction in the SIC (Fig. 1d) increases the ocean surface area that is exposed to the cold atmosphere. This 'area' effect overcompensates for the reduced heat loss due to a weakened air–sea surface temperature contrast and promotes an enhanced net heat loss to the atmosphere over the NENA (Supplementary Fig. 2b,c). As a consequence, the warmer SAT enhances the local cyclonic wind stress that strengthens the North Atlantic Subpolar Gyre (Fig. 2e and Supplementary Fig. 2a,e). This in turn strengthens local sea-ice variability, shifting its probability distribution from a single peak to a double peak prior to the AMOC resumption (Supplementary Fig. 10). It is important to note that a sea-ice-free mode already exists in the key convection sites of the North Atlantic, as the AMOC is still in its weak mode. Therefore, we infer that changes in SIC alone are not the final trigger for the AMOC recovery. Once the AMOC recovery is triggered by changes in large-scale salinity advection, the atmospheric responses associated with the sea-ice reduction will boost a northward transport of surface water with a relatively high salinity from the south-eastern subpolar regions to the convection sites (Fig. 2b and Supplementary Figs 2d and 11). This deepens vertical mixing with underlying warmer water masses in the NENA, leading to an additional reduction in the SIC (Fig. 1e and Supplementary Fig. 2a,f). The positive local atmosphere–ocean–sea-ice feedback mechanisms superposed on the larger-scale salinity advection feedback operate to abruptly return NADW formation to a vigorous interstadial mode from cold stadial conditions as atmospheric CO_2 increases.

AMOC response to CO_2 change in the presence of hosing

The characteristic mechanisms and feedbacks that occur in response to CO_2 changes, leading to shifts in the mode of AMOC, also operate in the presence of positive freshwater perturbations to the

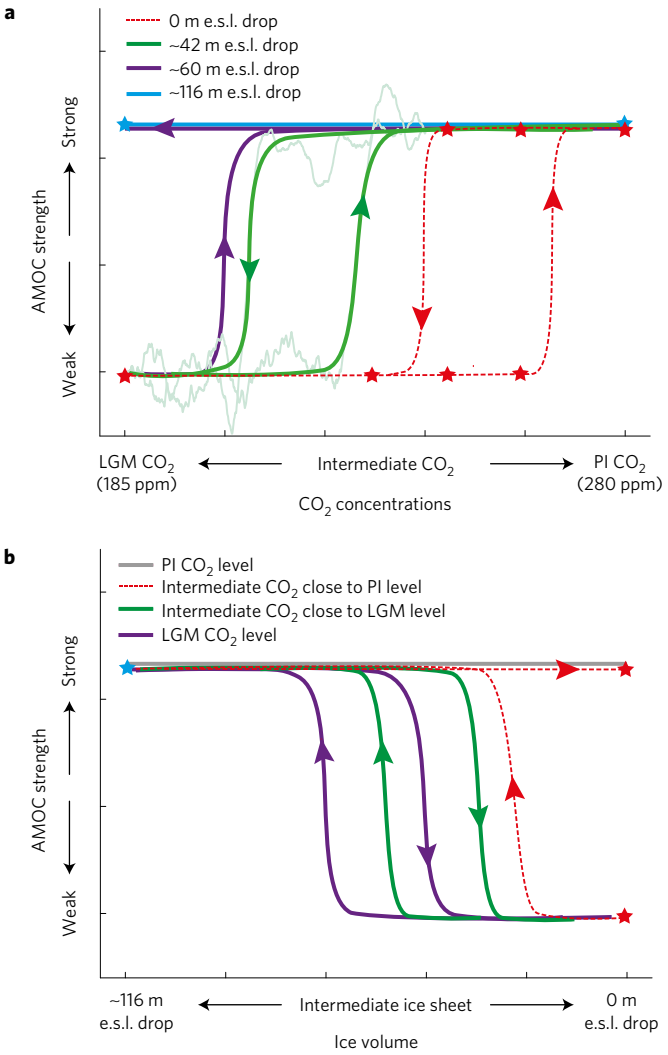

Figure 4 | Synthesis of AMOC stability diagrams. a, CO_2 change-induced diagram under different constant global ice volumes. The colour scheme represents scenarios with different ice-volume levels expressed as equivalent sea-level (e.s.l.) drops. **b**, Ice-volume change-induced diagram under different constant CO_2 levels. The colour scheme represents scenarios with different CO_2 levels. The faint green curve in **a** represents experiment CO2_Hys, identical to Fig. 2a. Stars are indicative of equilibrium simulations (Supplementary Table 1) and solid lines represent hysteresis behaviour in response to gradual changes in atmospheric CO_2 in **a** and ice volume in **b**. Dashed lines in **a** and **b** represent inferred changes in AMOC strength based on equilibrium simulations performed in this study and refs 8,9. PI, pre-industrial.

North Atlantic (experiment LGM_0.15_CO2) (Fig. 1h–n, and Supplementary Figs 12 and 13). This indicates that the proposed mechanism can overcome the negative effect of persistent NA freshwater input on AMOC strength after a CO_2 increase of ~40 ppm from the peak glacial level (185 ppm), ultimately triggering an abrupt warming in the North Atlantic (perhaps analogous to the sequence of events leading to the Bølling–Allerød (BA) and earlier Heinrich stadial–interstadial transitions). This further adds credence to the robustness of our results that are derived from the model without ice sheet dynamics, since diagnosed meltwater fluxes associated with changes in surface mass balance of the ice sheet are around 0.06 Sv during the interval A–B of experiment CO2_Hys. In addition, AMOC variability is characterized by increasing variance and autocorrelation in experiment LGM_0.15_CO2 as the threshold is approached during the transition from a strong to a weak AMOC mode (Fig. 1h–n). This feature, although shorter than non-Heinrich–DO events during Marine Isotope Stage (MIS) 3 (for example, DO events 5–7) (ref. 1), provides a potential approach to explain their occurrence[39], but requires further investigation in the future.

AMOC stability and glacial climate

In contrast to previous studies[22,23], the model used in this study, with more advanced climate physics, enables us to elaborate on the comprehensive dynamics of mechanisms associated with changes in atmospheric CO_2 to explain millennial-scale variability and abrupt climate transitions during glacial periods. As a consequence of CO_2 changes, variations in the freshwater budget of the North Atlantic associated with the interoceanic atmospheric moisture transport across Central America represent a crucial control for the stability of glacial climate by providing a natural source of 'freshwater perturbation' to the North Atlantic, thereby complementing previous concepts[5].

In combination with previous knowledge of the stability of the glacial climate[5,8], we synthesize a concept to account for a broader spectrum of abrupt climate changes as documented in global climate archives (Fig. 4). As shown in the conceptual AMOC stability diagrams, both LGM ice volume and interglacial atmospheric CO_2 concentrations are accompanied by a strong mono-stable AMOC, reflecting the dominant role of ice volume under peak glacial conditions and atmospheric CO_2 during interglacial periods (Fig. 4). The interplay between changes in ice volume and atmospheric CO_2 therefore determines that windows of AMOC bi-stability will exist during intermediate conditions between peak glacial and interglacial states. For example, MIS 3 was characterized by pronounced millennial-scale climate activity, whereas the LGM and Holocene interglacial were not. Only within a window of bi-stability can temporary perturbations (for example, CO_2, freshwater, solar irradiance, and so on) have a longer-term persistent effect on climate beyond the duration of the perturbation itself. Importantly, our analysis also shows that gradual changes in atmospheric CO_2 can act as a trigger of abrupt climate changes. Moreover, because millennial-scale changes in CO_2 are themselves thought to be driven in part by changes in the AMOC (with a weakened AMOC giving rise to a gradual rise in CO_2 and vice versa)[40], our results suggest that CO_2 might represent an internal feedback agent to AMOC changes[19] by promoting spontaneous transitions between contrasting climate states without the need for processes such as ice-rafting events across the North Atlantic[15,18]. More specifically, such an internal link can be characterized by rising CO_2 during Heinrich Stadial cold events, triggering abrupt transitions to warm conditions, and decreasing CO_2 during warm events, leading to abrupt cooling transitions. Therefore, CO_2 might provide a negative feedback on AMOC-induced climate shifts. We note that this mechanism may not account for non-H–DO variability, although feasibly an analogous process may be at work for these 'smaller' events[18,19].

Our framework also indicates that during deglaciation the bi-stable window would be established only after ice volume has started to decrease, but before peak interglacial CO_2 levels are achieved. For example, recovery of the AMOC during the BA warming occurred relatively early within Termination 1 (T1), before atmospheric CO_2 had attained its interglacial level and while the system was within its window of bi-stability, thus enabling a return to a weak mode of AMOC during the Younger Dryas (YD). By analogy, during glacial inception a bi-stable AMOC regime only occurs after atmospheric CO_2 has declined from peak interglacial CO_2 levels and before ice volume has reached full glacial values.

Although the exact position of the simulated bi-stable AMOC windows with respect to ice volume[8] and atmospheric CO_2 might be different among climate models, the combined framework that

is derived from our model can provide a systemic understanding of their relative roles within glacial–interglacial cycles (Fig. 4). In future studies of glacial–interglacial and millennial-scale climate variability, the processes and feedbacks invoked here might serve as a basis to identify principal triggering mechanisms and forcing agents in both high-resolution climate records and coupled climate model simulations that include carbon cycle dynamics and interactive ice sheet components.

Methods

Methods, including statements of data availability and any associated accession codes and references, are available in the online version of this paper.

Received 6 February 2017; accepted 23 May 2017; published online 19 June 2017

References

1. Dansgaard, W. *et al*. Evidence for general instability of past climate from a 250-kyr ice-core record. *Nature* **364,** 218–220 (1993).
2. Barker, S. *et al*. 800,000 years of abrupt climate variability. *Science* **334,** 347–351 (2011).
3. Rahmstorf, S. Ocean circulation and climate during the past 120,000 years. *Nature* **419,** 207–214 (2002).
4. Stommel, H. Thermohaline convection with two stable regimes of flow. *Tellus* **13,** 224–230 (1961).
5. Ganopolski, A. & Rahmstorf, S. Rapid changes of glacial climate simulated in a coupled climate model. *Nature* **409,** 153–158 (2001).
6. McManus, J. F., Oppo, D. W. & Cullen, J. L. A 0.5-million-year record of millennial-scale climate variability in the North Atlantic. *Science* **283,** 971–975 (1999).
7. Wunsch, C. Abrupt climate change: an alternative view. *Quat. Res.* **65,** 191–203 (2006).
8. Zhang, X., Lohmann, G., Knorr, G. & Purcell, C. Abrupt glacial climate shifts controlled by ice sheet changes. *Nature* **512,** 290–294 (2014).
9. Zhang, X., Lohmann, G., Knorr, G. & Xu, X. Different ocean states and transient characteristics in Last Glacial Maximum simulations and implications for deglaciation. *Clim. Past* **9,** 2319–2333 (2013).
10. Menviel, L., Timmermann, A., Friedrich, T. & England, M. H. Hindcasting the continuum of Dansgaard–Oeschger variability: mechanisms, patterns and timing. *Clim. Past* **10,** 63–77 (2014).
11. Hemming, S. Heinrich events: massive Late Pleistocene detritus layers of the North Atlantic and their global climate imprint. *Rev. Geophys.* **42,** RG1005 (2004).
12. Marcott, S. A. *et al*. Ice-shelf collapse from subsurface warming as a trigger for Heinrich events. *Proc. Natl Acad. Sci. USA* **108,** 13415–13419 (2011).
13. Bassis, J. N., Petersen, S. V. & Mac Cathles, L. Heinrich events triggered by ocean forcing and modulated by isostatic adjustment. *Nature* **542,** 332–334 (2017).
14. Bond, G. *et al*. A pervasive millennial-scale cycle in North Atlantic Holocene and glacial climates. *Science* **278,** 1257–1266 (1997).
15. Barker, S. *et al*. Icebergs not the trigger for North Atlantic cold events. *Nature* **520,** 333–336 (2015).
16. Jouzel, J. *et al*. Orbital and millennial Antarctic climate variability over the past 800,000 years. *Science* **317,** 793–796 (2007).
17. Stocker, T. F. & Johnsen, S. J. A minimum thermodynamic model for the bipolar seesaw. *Paleoceanography* **18,** 1–9 (2003).
18. Barker, S. & Knorr, G. A paleo-perspective on the AMOC as a tipping element. *PAGES News* **24,** 14–15 (2016).
19. Barker, S. & Knorr, G. Antarctic climate signature in the Greenland ice core record. *Proc. Natl Acad. Sci. USA* **104,** 17278–17282 (2007).
20. Bereiter, B. *et al*. Revision of the EPICA Dome C CO_2 record from 800 to 600 kyr before present. *Geophys. Res. Lett.* **42,** 1–8 (2015).
21. Kawamura, K. *et al*. State dependence of climatic instability over the past 720,000 years from Antarctic ice cores and climate modeling. *Sci. Adv.* **3,** 1–14 (2017).
22. Knorr, G. & Lohmann, G. Rapid transitions in the Atlantic thermohaline circulation triggered by global warming and meltwater during the last deglaciation. *Geochem. Geophys. Geosyst.* **8,** Q12006 (2007).
23. Banderas, R., Alvarez-Solas, J., Robinson, A. & Montoya, M. An interhemispheric mechanism for glacial abrupt climate change. *Clim. Dynam.* **44,** 2897–2908 (2014).
24. Ahn, J. & Brook, E. J. Siple Dome ice reveals two modes of millennial CO_2 change during the last ice age. *Nat. Commun.* **5,** 3723 (2014).
25. Grant, K. M. *et al*. Rapid coupling between ice volume and polar temperature over the past 150,000 years. *Nature* **491,** 744–747 (2012).
26. Marcott, S. A. *et al*. Centennial-scale changes in the global carbon cycle during the last deglaciation. *Nature* **514,** 616–619 (2014).
27. Li, C., Battisti, D. S. & Bitz, C. M. Can North Atlantic Sea ice anomalies account for Dansgaard–Oeschger climate signals? *J. Clim.* **23,** 5457–5475 (2010).
28. Peterson, L. C., Haug, G. H., Hughen, K. A. & Roehl, U. Rapid changes in the hydrologic cycle of the tropical Atlantic during the last glacial. *Science* **290,** 1947–1951 (2000).
29. Voelker, A. H. L. Global distribution of centennial-scale records for Marine Isotope Stage (MIS) 3: a database. *Quat. Sci. Rev.* **21,** 1185–1212 (2002).
30. Lohmann, G. Atmospheric and oceanic freshwater transport during weak Atlantic overturning circulation. *Tellus* **5,** 438–449 (2003).
31. Rahmstorf, S. On the freshwater forcing and transport of the Atlantic thermohaline circulation. *Clim. Dynam.* **12,** 799–811 (1996).
32. Knorr, G. & Lohmann, G. Southern Ocean origin for the resumption of Atlantic thermohaline circulation during deglaciation. *Nature* **424,** 532–536 (2003).
33. Broecker, W. S., Bond, G., Klas, M., Bonani, G. & Wolfli, W. A salt oscillator in the glacial Atlantic? 1. The concept. *Paleoceanography* **5,** 469–477 (1990).
34. Schmidt, M. W., Vautravers, M. J. & Spero, H. J. Rapid subtropical North Atlantic salinity oscillations across Dansgaard–Oeschger cycles. *Nature* **443,** 561–564 (2006).
35. Zaucker, F. & Broecker, W. S. The influence of atmospheric moisture transport on the fresh water balance of the Atlantic drainage basin: general circulation model simulations and observations. *J. Geophys. Res.* **97,** 2765–2773 (1992).
36. Collins, M. *et al*. in *Climate Change 2013: The Physical Science Basis* (eds Stocker, T. F. *et al*.) 1029–1136 (IPCC, Cambridge Univ. Press, 2013).
37. Ahn, J. & Brook, E. J. Atmospheric CO_2 and climate on millennial time scales during the last glacial period. *Science* **83,** 83–85 (2008).
38. Leduc, G. *et al*. Moisture transport across Central America as a positive feedback on abrupt climatic changes. *Nature* **445,** 908–911 (2007).
39. Peltier, W. R. & Vettoretti, G. Dansgaard-Oeschger oscillations predicted in a comprehensive model of glacial climate: a 'kicked' salt oscillator in the Atlantic. *Geophys. Res. Lett.* **41,** 7306–7313 (2014).
40. Schmittner, A. & Galbraith, E. D. Glacial greenhouse-gas fluctuations controlled by ocean circulation changes. *Nature* **456,** 373–376 (2008).

Acknowledgements

X.Z. thanks G. Leduc for helpful discussion about marine sediment core MD02-2529. We thank colleagues in the Paleoclimate Dynamics group at the Alfred Wegener Institute Helmholtz Center for Polar and Marine Research (AWI) in Bremerhaven for general support and the AWI Computer Centre for keeping the supercomputer running. This study is supported by Helmholtz Postdoc Programme (PD-301), as well as the PACES program of the AWI and the BMBF funded project PalMod. The opening foundations of the Key Laboratory of Marine Sedimentology & Environmental Geology, SOA, (grant No. MASEG201701) and State Key Laboratory of Marine Geology, Tongji University (grant No. MGK1611) as well as the national Natural Science Foundation of China (grant No. 41575067) are grateful acknowledged (X.Z.). Furthermore, G.K. acknowledges funding by 'Helmholtz Climate Initiative REKLIM' (Regional Climate Change), a joint research project of the Helmholtz Association of German research centres (HGF). We also acknowledge financial support from the UK NERC (grants NE/J008133/1 and NE/L006405/1) to S.B.

Author contributions

All authors conceived the study. X.Z. designed and performed the model simulations, analysed the results, and led the write up of the manuscript with G.K. All authors interpreted the results and contributed to the final version of the manuscript.

Additional information

Supplementary information is available in the online version of the paper. Reprints and permissions information is available online at www.nature.com/reprints. Publisher's note: Springer Nature remains neutral with regard to jurisdictional claims in published maps and institutional affiliations. Correspondence and requests for materials should be addressed to X.Z.

Competing financial interests

The authors declare no competing financial interests.

Methods

We use a comprehensive fully coupled atmosphere–ocean general circulation model (AOGCM), COSMOS (ECHAM5-JSBACH-MPI-OM) for this study. The atmospheric model ECHAM5 (ref. 41), complemented by a land surface component JSBACH[42], is used at T31 resolution (∼3.75°), with 19 vertical layers. The ocean model MPI-OM[43], including sea-ice dynamics that is formulated using viscous-plastic rheology[44], has a resolution of GR30 ($3^\circ \times 1.8^\circ$) in the horizontal, with 40 uneven vertical layers. The climate model has already been used to simulate the past millennium[45], the Miocene warm climate[46,47], the Pliocene[48], the internal variability of the climate system[49], Holocene variability[50], the Last Glacial Maximum (LGM) climate[9,51] and glacial millennial-scale variability[8,52,53]. To evaluate the role of atmospheric CO_2 on the AMOC stability, boundary conditions including ice sheet extent, topography over bare land, orbital configuration, land sea mask, bathymetry, CH_4 and N_2O, are fixed to the LGM. Note that the imposed ice sheet heights in experiment CO2_Hys and LGM_0.15_CO2 are different. In experiment CO2_Hys the ice volume is equivalent to an approximately 40 m sea-level drop, while it is identical to the LGM in experiment LGM_0.15_CO2. The ocean states under both ice sheet configurations are characterized by only one stable AMOC mode[8], which enable us verify whether changes in atmospheric CO_2 do play a role on AMOC hysteresis.

Code availability. The standard model code of the 'Community Earth System Models' (COSMOS) version COSMOS-landveg r2413 (2009) is available upon request from the 'Max Planck Institute for Meteorology' in Hamburg (https://www.mpimet.mpg.de).

Data availability. The data used in this paper are available at the following sources. Bereiter *et al.* (2015), CO_2 data: http://onlinelibrary.wiley.com/store/10.1002/2014GL061957/asset/supinfo/grl52461-sup-0003-supplementary.xls?v=1&s=e77ad89c3925111330671009ab40eac65e019d01. Leduc *et al.* (2007), salinity reconstruction in the eastern equatorial Pacific: ftp://ftp.ncdc.noaa.gov/pub/data/paleo/contributions_by_author/leduc2007/leduc2007.txt. The model data that support the findings of this study are available from the corresponding author upon reasonable request.

References

41. Roeckner, E. *et al*. *The Atmospheric General Circulation Model ECHAM5. Part 1: Model Description* Report No. 349, 1–127 (Max-Planck-Institut fuer Meteorologie, 2003).
42. Brovkin, V., Raddatz, T., Reick, C. H., Claussen, M. & Gayler, V. Global biogeophysical interactions between forest and climate. *Geophys. Res. Lett.* **36,** 1–5 (2009).
43. Marsland, S. J., Haak, H., Jungclaus, J. H., Latif, M. & Röske, F. The Max-Planck-Institute global ocean/sea ice model with orthogonal curvilinear coordinates. *Ocean Model.* **5,** 91–127 (2003).
44. Hibler, W. III A dynamic thermodynamic sea ice model. *J. Phys. Oceanogr.* **9,** 815–846 (1979).
45. Jungclaus, J. H. *et al*. Climate and carbon-cycle variability over the last millennium. *Clim. Past* **6,** 723–737 (2010).
46. Knorr, G., Butzin, M., Micheels, A. & Lohmann, G. A warm Miocene climate at low atmospheric CO_2 levels. *Geophys. Res. Lett.* **38,** 1–5 (2011).
47. Knorr, G. & Lohmann, G. Climate warming during Antarctic ice sheet expansion at the Middle Miocene transition. *Nat. Geosci.* **7,** 2–7 (2014).
48. Stepanek, C. & Lohmann, G. Modelling mid-Pliocene climate with COSMOS. *Geosci. Model Dev.* **5,** 1221–1243 (2012).
49. Wei, W., Lohmann, G. & Dima, M. Distinct modes of internal variability in the Global Meridional Overturning Circulation associated with the Southern Hemisphere westerly winds. *J. Phys. Oceanogr.* **42,** 785–801 (2012).
50. Wei, W. & Lohmann, G. Simulated Atlantic multidecadal oscillation during the Holocene. *J. Clim.* **25,** 6989–7022 (2012).
51. Abelmann, A. *et al*. The seasonal sea-ice zone in the glacial Southern Ocean as a carbon sink. *Nat. Commun.* **6,** 8136 (2015).
52. Gong, X., Knorr, G., Lohmann, G. & Zhang, X. Dependence of abrupt Atlantic meridional ocean circulation changes on climate background states. *Geophys. Res. Lett.* **40,** 3698–3704 (2013).
53. Köhler, P., Knorr, G. & Bard, E. Permafrost thawing as a possible source of abrupt carbon release at the onset of the Bølling/Allerød. *Nat. Commun.* **5,** 5520 (2014).